Research Article | Vol. 26, No. 4 | 19 Feb 2018 | OPTICS EXPRESS 4961
Optics EXPRESS

Tm:$KY_{1-x-y}Gd_xLu_y(WO_4)_2$ planar waveguide laser passively Q-switched by single-walled carbon nanotubes

ESROM KIFLE,[1] XAVIER MATEOS,[1,*] PAVEL LOIKO,[2] SUN YUNG CHOI,[3] JI EUN BAE,[3] FABIAN ROTERMUND,[3] MAGDALENA AGUILÓ,[1] FRANCESC DÍAZ,[1] UWE GRIEBNER,[4] AND VALENTIN PETROV[4]

[1]*Física i Cristal·lografia de Materials i Nanomaterials (FiCMA-FiCNA)-EMaS, Dept. Química Física i Inòrganica, Universitat Rovira i Virgili (URV), Campus Sescelades, E-43007 Tarragona, Spain*
[2]*ITMO University, 49 Kronverkskiy pr., 197101 St. Petersburg, Russia*
[3]*Department of Physics, KAIST, 291 Daehak-ro, Yuseong-gu, 34141 Daejeon, South Korea*
[4]*Max Born Institute for Nonlinear Optics and Short Pulse Spectroscopy, Max-Born-Str. 2a, D-12489 Berlin, Germany*
[*]*xavier.mateos@urv.cat*

Abstract: A Tm^{3+} monoclinic double tungstate planar waveguide laser is passively Q-switched (PQS) by a saturable absorber (SA) based on single-walled carbon nanotubes (SWCNTs) randomly oriented in a polymer film. The laser is based on a 18 µm-thick 5 at.% Tm:$KY_{1-x-y}Gd_xLu_y(WO_4)_2$ active layer grown on an undoped (010)-oriented $KY(WO_4)_2$ substrate by liquid phase epitaxy with determined propagation losses 0.7 ± 0.2 dB/cm. The PQS laser generated a maximum average output power of 45.6 mW at 1.8354 µm with a slope efficiency of 22.5%. Stable 83-ns-long laser pulses with an energy of 33 nJ were achieved at a repetition rate of 1.39 MHz. The use of SWCNTs as SA is promising for generation of sub-100 ns pulses in such waveguide lasers at ~2 µm.

OCIS codes: (140.3380) Laser materials; (230.7390) Waveguides, planar; (140.3540) Lasers, Q-switched.

References and links

1. W. B. Cho, J. H. Yim, S. Y. Choi, S. Lee, A. Schmidt, G. Steinmeyer, U. Griebner, V. Petrov, D.-I. Yeom, K. Kim, and F. Rotermund, "Boosting the nonlinear optical response of carbon nanotube saturable absorbers for broadband mode-locking of bulk lasers," Adv. Funct. Mater. **20**(12), 1937–1943 (2010).
2. W. B. Cho, A. Schmidt, J. H. Yim, S. Y. Choi, S. Lee, F. Rotermund, U. Griebner, G. Steinmeyer, V. Petrov, X. Mateos, M. C. Pujol, J. J. Carvajal, M. Aguiló, and F. Díaz, "Passive mode-locking of a Tm-doped bulk laser near 2 µm using a carbon nanotube saturable absorber," Opt. Express **17**(13), 11007–11012 (2009).
3. R. Lan, P. Loiko, X. Mateos, Y. Wang, J. Li, Y. Pan, S. Y. Choi, M. H. Kim, F. Rotermund, A. Yasukevich, K. Yumashev, U. Griebner, and V. Petrov, "Passive Q-switching of microchip lasers based on Ho:YAG ceramics," Appl. Opt. **55**(18), 4877–4887 (2016).
4. P. Loiko, X. Mateos, S. Y. Choi, F. Rotermund, J. M. Serres, M. Aguiló, F. Díaz, K. Yumashev, U. Griebner, and V. Petrov, "Vibronic thulium laser at 2131 nm Q-switched by single-walled carbon nanotubes," J. Opt. Soc. Am. B **33**(11), D19–D27 (2016).
5. X. Mateos, P. Loiko, S. Y. Choi, F. Rotermund, M. Aguiló, F. Díaz, U. Griebner, and V. Petrov, "Single-walled carbon nanotubes oust graphene and semiconductor saturable absorbers in Q-switched solid-state lasers at 2 µm," Laser Phys. Lett. **14**(9), 095801 (2017).
6. K. van Dalfsen, S. Aravazhi, D. Geskus, K. Wörhoff, and M. Pollnau, "Efficient $KY_{1-x-y}Gd_xLu_y(WO_4)_2$:$Tm^{3+}$ channel waveguide lasers," Opt. Express **19**(6), 5277–5282 (2011).
7. W. Bolanos, F. Starecki, A. Benayad, G. Brasse, V. Ménard, J.-L. Doualan, A. Braud, R. Moncorgé, and P. Camy, "Tm:$LiYF_4$ planar waveguide laser at 1.9 µm," Opt. Lett. **37**(19), 4032–4034 (2012).
8. D. G. Lancaster, S. Gross, H. Ebendorff-Heidepriem, K. Kuan, T. M. Monro, M. Ams, A. Fuerbach, and M. J. Withford, "Fifty percent internal slope efficiency femtosecond direct-written Tm^{3+}:ZBLAN waveguide laser," Opt. Lett. **36**(9), 1587–1589 (2011).
9. J. I. Mackenzie, S. C. Mitchell, R. J. Beach, H. E. Meissner, and D. P. Shepherd, "15 W diode-side-pumped TmYAG waveguide laser at 2 µm," Electron. Lett. **37**(14), 898–899 (2001).
10. K. van Dalfsen, S. Aravazhi, C. Grivas, S. M. García-Blanco, and M. Pollnau, "Thulium channel waveguide laser with 1.6 W of output power and ~80% slope efficiency," Opt. Lett. **39**(15), 4380–4383 (2014).
11. W. Bolaños, J. J. Carvajal, X. Mateos, E. Cantelar, G. Lifante, U. Griebner, V. Petrov, V. L. Panyutin, G. S. Murugan, J. S. Wilkinson, M. Aguiló, and F. Díaz, "Continuous-wave and Q-switched Tm-doped $KY(WO_4)_2$ planar waveguide laser at 1.84 µm," Opt. Express **19**(2), 1449–1454 (2011).

#314811 https://doi.org/10.1364/OE.26.004961
Journal © 2018 Received 1 Dec 2017; revised 25 Jan 2018; accepted 27 Jan 2018; published 16 Feb 2018

Optics EXPRESS

12. J. H. Lee, S. Gross, B. V. Cunning, C. L. Brown, D. Kielpinski, T. M. Monro, and D. G. Lancaster, "Graphene-based passive Q-switching of a Tm^{3+}:ZBLAN short-infrared waveguide laser," in *Conference on Lasers and Electro-Optics (CLEO)* (IEEE, 2014), paper P. JTu4A.128.
13. Y. Ren, G. Brown, R. Mary, G. Demetriou, D. Popa, F. Torrisi, A. C. Ferrari, F. Chen, and A. K. Kar, "7.8-GHz graphene-based 2-μm monolithic waveguide laser," IEEE J. Sel. Top. Quantum Electron. **21**(1), 395–400 (2015).
14. E. Kifle, X. Mateos, J. R. de Aldana, A. Ródenas, P. Loiko, S. Y. Choi, F. Rotermund, U. Griebner, V. Petrov, M. Aguiló, and F. Díaz, "Femtosecond-laser-written Tm:$KLu(WO_4)_2$ waveguide lasers," Opt. Lett. **42**(6), 1169–1172 (2017).
15. V. Petrov, M. C. Pujol, X. Mateos, Ò. Silvestre, S. Rivier, M. Aguiló, R. M. Solé, J. H. Liu, U. Griebner, and F. Díaz, "Growth and properties of $KLu(WO_4)_2$, and novel ytterbium and thulium lasers based on this monoclinic crystalline host," Laser Photonics Rev. **1**(2), 179–212 (2007).
16. S. Aravazhi, D. Geskus, K. van Dalfsen, S. A. Vázquez-Córdova, C. Grivas, U. Griebner, S. M. García-Blanco, and M. Pollnau, "Engineering lattice matching, doping level, and optical properties of $KY(WO_4)_2$:Gd,Lu,Yb layers for a cladding-side-pumped channel waveguide laser," Appl. Phys. B **111**(3), 433–446 (2013).
17. W. Bolaños, J. J. Carvajal, M. C. Pujol, X. Mateos, G. Lifante, M. Aguiló, and F. Díaz, "Epitaxial growth of lattice matched $KY_{1-x-y}Gd_xLu_y(WO_4)_2$ thin films on $KY(WO_4)_2$ substrates for waveguiding applications," Cryst. Growth Des. **9**(8), 3525–3531 (2009).
18. J. Morris, N. K. Stevenson, H. T. Bookey, A. K. Kar, C. T. A. Brown, J.-M. Hopkins, M. D. Dawson, and A. A. Lagatsky, "1.9 μm waveguide laser fabricated by ultrafast laser inscription in Tm:Lu_2O_3 ceramic," Opt. Express **25**(13), 14910–14917 (2017).
19. P. K. Tien and R. Ulrich, "Theory of prism–film coupler and thin-film light guides," J. Opt. Soc. Am. **60**(10), 1325–1337 (1970).
20. A. S. Yasukevich, P. Loiko, N. V. Gusakova, J. M. Serres, X. Mateos, K. V. Yumashev, N. V. Kuleshov, V. Petrov, U. Griebner, M. Aguiló, and F. Díaz, "Modeling of graphene Q-switched Tm lasers," Opt. Commun. **389**, 15–22 (2017).
21. J. M. Serres, P. Loiko, X. Mateos, K. Yumashev, U. Griebner, V. Petrov, M. Aguiló, and F. Díaz, "Tm:$KLu(WO_4)_2$ microchip laser Q-switched by a graphene-based saturable absorber," Opt. Express **23**(11), 14108–14113 (2015).
22. X. Jiang, S. Gross, H. Zhang, Z. Guo, M. J. Withford, and A. Fuerbach, "Bismuth telluride topological insulator nanosheet saturable absorbers for q-switched mode-locked Tm:ZBLAN waveguide lasers," Ann. Phys. **528**(7–8), 543–550 (2016).
23. E. Kifle, X. Mateos, P. Loiko, K. Yumashev, A. Yasukevich, V. Petrov, U. Griebner, M. Aguiló, and F. Díaz, "Graphene Q-switched Tm:$KY(WO_4)_2$ waveguide laser," Laser Phys. **27**(4), 045801 (2017).

1. Introduction

Single-walled carbon nanotubes (SWCNTs) representing rolled sheets of graphene are emerging as broadband saturable absorbers (SAs) for passively Q-switched (PQS) and mode-locked lasers at 1-2 μm [1,2]. They exhibit relatively low saturation intensity, ultrafast recovery time of the initial absorption, high fraction of saturable loss and acceptable laser damage threshold [1–3]. Recently, SWCNT-SAs have been employed in compact 2-μm PQS bulk lasers based on Tm^{3+} or Ho^{3+} active ions, generating sub-100 ns pulses at high repetition rates approaching the MHz-range [3,4]. The performance of SWCNT-SAs in such lasers has proved to be superior to graphene-SAs and commercial semiconductor SAs [5].

Waveguide lasers emitting at ~2 μm are of interest for environmental and medical sensing applications. To date, multiple studies focused on continuous-wave (CW) planar and channel Tm-doped waveguide lasers [6–9] including such featuring very high laser efficiency [10]. Only few reports on passive Q-switching of such waveguide lasers can be found [11–14], mostly due to the lack of suitable SAs in the 2-μm spectral range. The required SAs should exhibit low insertion losses, high modulation depth and low saturation intensity. In the present paper, we report on the successful application of SWCNT-SAs in a PQS planar waveguide laser based on a Tm^{3+}-doped monoclinic double tungstate (MDT) epitaxial structure, Tm:$KY_{1-x-y}Gd_xLu_y(WO_4)_2$ / $KY(WO_4)_2$. Tm^{3+}-doped MDTs are known for their excellent spectroscopic properties [15], a prerequisite for high laser efficiency in waveguide lasers [10].

2. Experimental

The active layer with a composition $KY_{0.61}Gd_{0.22}Lu_{0.12}Tm_{0.05}(WO_4)_2$ (abbreviated: 5 at. % Tm:KYW, Tm^{3+} concentration: $N_{Tm} = 2.9 \times 10^{20}$ cm^{-3}) was grown by the liquid phase epitaxy (LPE) method on a (010)-oriented bulk substrate of an undoped $KY(WO_4)_2$ (KYW) crystal. A "mixed" active layer (i.e., incorporating Y^{3+}, Gd^{3+} and Lu^{3+} "passive"

Optics EXPRESS

ions) was used in order to reach simultaneously good lattice matching and high refractive index contrast with respect to the substrate [16,17]. The bulk crystal used as a substrate was grown by the Top-Seeded Solution Growth (TSSG) Slow-Cooling method using a [010]-oriented seed [15]. In both cases, potassium ditungstate, $K_2W_2O_7$, was used as a solvent. The solute/solvent ratio was 12/88 mol% and 7/93 mol% for the growth of the substrate and the epitaxial layer, respectively. The saturation temperature for the active layer T_S was 1160.7 K. During the LPE growth processes, ~8.0 mm of the substrate was vertically dipped into the solution while being rotated at 10 rev/min. The growth process took 3 hours at 3 K below T_S. Subsequently, the epitaxial layer was polished down to 18 μm thickness, Fig. 1(a). The sample was prepared for light propagation along the N_g optical indicatrix axis of the biaxial KYW. The refractive index contrast between the epitaxial layer and the substrate was estimated at the laser wavelength of ~1.84 μm using the Sellmeier equations [16] as Δn ~0.004 (for light polarization $E \parallel N_m$). The two end facets of the epitaxial structure were polished to laser quality, resulting in a final waveguide length l of 5.0 mm.

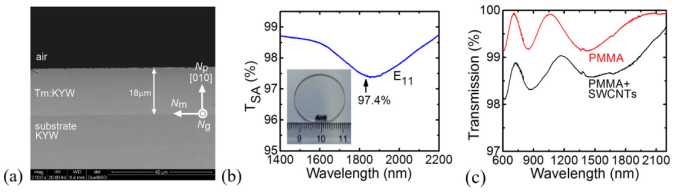

Fig. 1. (a) Environmental-SEM back-scattering image of the polished end-facet of the Tm:KYW/KYW epitaxy; (b) initial small-signal transmission of the SWCNT-SA (Fresnel losses are subtracted), *inset* – image of the SA. *Arrow* denotes the laser wavelength (PQS laser); (c) small-signal transmission spectra of SWCNT/PMMA and pure PMMA films of the same thickness (~200 nm).

The SWCNTs were synthesized by the arc-discharge technique with diameters spanning from 1.3 up to 1.5 nm. The SWCNT/PMMA (polymethylmethacrylate) mixture was spin-coated onto an uncoated 1-mm thick quartz substrate, wherein the individual SWCNTs exhibited a random (spaghetti-like) orientation [1,4]. The thickness of the coated SWCNT/PMMA layer was ~300 nm. The internal small-signal transmission spectrum of the SA shows a broad absorption band spanning from 1.6 to 2.2 μm, which is related to the first fundamental electronic transition of semiconducting carbon nanotubes (E_{11}), Fig. 1(b). The small-signal transmission T_{SA} of the SA was 97.4% at 1.84 μm. The saturation intensity I_S of a similar SA was estimated in [3] as ~7 MW/cm^2 and the fraction of the saturable losses α'_S/α' ~0.21 (in the 2 μm spectral range) [3], so that the modulation depth of the utilized SA at the laser wavelength was ~0.54%.

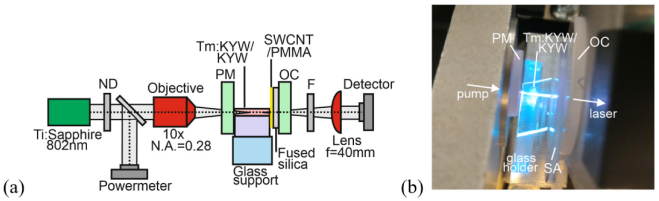

Fig. 2. (a) Scheme of the waveguide laser set-up: PM – pump mirror, OC – output coupler, ND – neutral density filter, F – long-pass filter; (b) blue upconversion luminescence from the PQS Tm:KYW planar waveguide laser.

To reveal the effect of PMMA on the linear absorption of the SA, we fabricated a similar SWCNT / PMMA film and an undoped PMMA film of the same thickness (~200 nm). Their small-signal transmission spectra are shown in Fig. 1(c). Both spectra contain similar interference-induced peaks and deeps while the transmission of the SWCNT / PMMA film is smaller. At a wavelength of 1.84 μm, the fraction of absorption due to the PMMA is minor (it is about 20%).

Optics EXPRESS

The scheme of the laser set-up is shown in Fig. 2(a). The Tm:KYW/KYW epitaxy was placed on a passively-cooled glass substrate. The laser cavity consisted of a flat pump mirror (PM) that was antireflection (AR) coated for 0.7–1 μm and high-reflection (HR) coated for 1.8–2.1 μm and a flat output coupler (OC) providing a transmission T_{OC} of 1.5%, 3%, 5%, 9%, 20% or 30% at 1.8–2.1 μm. A transmission-type SWCNT-SA was inserted between the waveguide and OC. All optical elements were placed as close as possible while avoiding the use of index-matching liquid. As pump source, a Ti:Sapphire laser tuned to 0.802 μm was used. A neutral density filter was applied to control the incident pump power. The polarization of the pump beam corresponded to $E \parallel N_m$ in the active layer. The pump was coupled into the waveguide by a 10 × microscope objective lens (numerical aperture, N.A.: 0.28, focal length: f = 20 mm) resulting in a spot radius of 20 μm. About 48 ± 3% of the incident pump power was launched into the active layer, as determined from the pump-transmission measurements out of the Tm^{3+} absorption. ~86-90% of the coupled light was absorbed under lasing conditions, as determined by a pump-transmission measurement under non-lasing conditions and rate-equation modelling. The unabsorbed residual pump was blocked with a long-pass filter (Thorlabs, FEL1000, transmission at the laser wavelength: ~83%) and the output laser beam was collimated with an aspherical plano-convex lens (f = 40 mm). The spectrum of the laser emission was measured using a Yokogawa optical spectrum analyser (OSA, model AQ6375B) and the beam profile was captured with a FIND-R-SCOPE near-IR camera.

3. Results and discussion

At first, we studied the continuous-wave (CW) operation of the Tm:KYW waveguide laser, shown in Figs. 3(a) and 3(b). The maximum output power of 154 mW was achieved for T_{OC} = 30% at 1.8392 μm corresponding to a slope efficiency η of 52.2% (with respect to the absorbed pump power P_{abs}). The laser threshold was at P_{abs} = 104 mW. Increasing the output coupling from 1.5% to 30%, the emission wavelength decreased from 1.8467 to 1.8392 μm due to the quasi-three level nature of the Tm^{3+} laser, Fig. 3(b). The active layer emitted blue upconversion luminescence from the Tm^{3+} ions ($^1G_4 \rightarrow {}^3H_6$ transition, centered at ~0.48 μm) as can be seen in Fig. 2(b). The propagation loss of the waveguide was estimated by applying the Caird analysis modified for high output coupling [18], $1/\eta = 1/\eta_0(1 + 2\gamma/\gamma_{OC})$, where $\gamma = -\ln(1 - L)$, L is the internal loss per pass, $\gamma_{OC} = -\ln(1 - T_{OC})$, and η_0 is the intrinsic slope efficiency. The Caird analysis is correct when the stimulated-emission cross-section is constant for the observed emission wavelengths. For Tm^{3+} ions in MDTs (for $E \parallel N_m$), its variation over 1.839-1.847 μm is minor [15]. From the linear fit shown in Fig. 3(c), values of η_0 = 59% and L = 0.08 ± 0.02 are deduced, so that the propagation loss $\delta = 4.34L/l$ amounts to 0.7 ± 0.2 dB/cm. This indicates a high quality of the active layer.

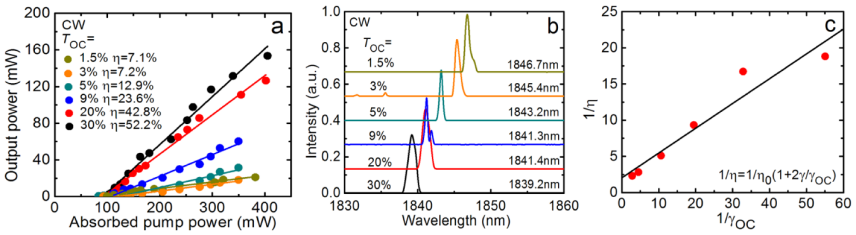

Fig. 3. CW Tm:KYW planar waveguide laser: (a) input-output dependences, η – slope efficiency; (b) typical laser emission spectra measured at maximum P_{abs}; (c) Caird analysis modified for high output coupling. The laser polarization is $E \parallel N_m$.

In the PQS operation mode, depicted in Fig. 4, the laser generated a maximum average output power of 45.6 mW at 1.8354 μm with η = 22.5% (for T_{OC} = 30%). The laser threshold was at P_{abs} = 150 mW and the conversion efficiency with respect to the CW operation mode η_{conv} was 29%. For lower T_{OC} = 20% and 9%, the laser slope efficiency was inferior: 16.3% and 8.3%, respectively. Further power scaling was limited by the available pump source. The emission wavelength slightly shortened with the

Optics EXPRESS

increase of T_{OC}, from 1.8371 to 1.8354 μm for the same reason as explained above for the CW regime, Fig. 4(b). The beam profile of the laser was slightly elliptic with a large extension in the non-guided plane of the waveguide, see inset of Fig. 4(a). According to the dispersion relation [19], the waveguide supports two transversal electric (TE) modes along the guided direction at a wavelength of ~1.84 μm. In both operation regimes, CW and PQS, the laser emission was linearly polarized, $E \parallel N_m$. The polarization was naturally-selected by the anisotropy of the gain.

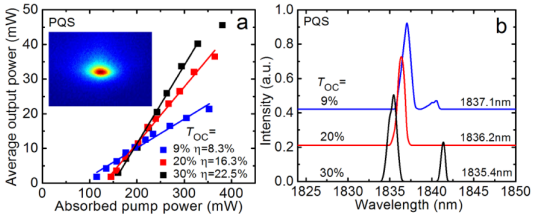

Fig. 4. SWCNT PQS Tm:KYW planar waveguide laser: (a) input-output dependences, η – slope efficiency; (b) typical laser emission spectra measured at maximum P_{abs}. The laser polarization is $E \parallel N_m$. *Inset* in (a) - far-field profile of the laser mode for T_{OC} = 30%, P_{abs} = 330 mW.

The pulse characteristics of the PQS Tm:KYW waveguide laser varied with P_{abs}. The pulse duration $\Delta\tau$ (determined as full width at half maximum, FWHM) decreased from 161 to 83 ns, the pulse energy E_{out} increased from 7.6 to 32.8 nJ and the pulse repetition frequency (PRF) increased almost linearly from 0.94 to 1.39 MHz when P_{abs} was increased from 176 to 381 mW (for T_{OC} = 30%), see Fig. 5. Such a behavior is typical for PQS lasers containing "fast" SAs and is related to the variable bleaching of the SA [20]. The shortest pulse duration (71 ns) corresponded to T_{OC} = 9% due to the higher intracavity peak intensity at the SA (~1.5 MW/cm^2). However, T_{OC} = 30% provided a higher pulse energy and, thus, the maximum peak power $P_{peak} = E_{out}/\Delta\tau$ reached 395 mW.

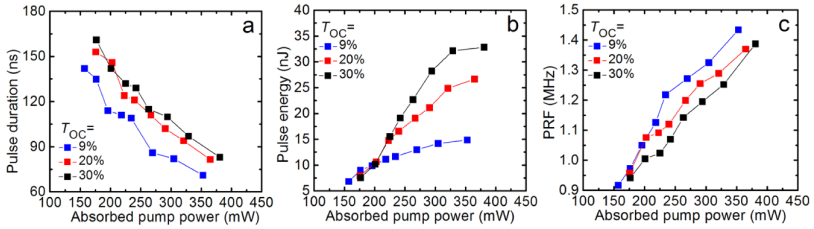

Fig. 5. SWCNT PQS Tm:KYW planar waveguide lasers: (a) pulse duration (FWHM), (b) pulse energy and (c) pulse repetition frequency (PRF) vs. absorbed pump power.

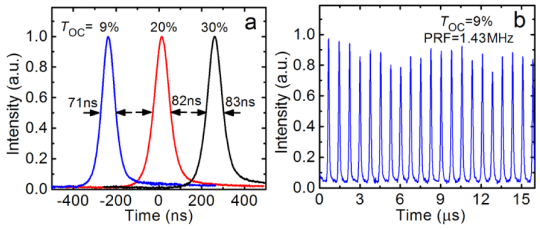

Fig. 6. Oscilloscope traces of the SWCNT PQS Tm:KYW planar waveguide laser output recorded by a fast InGaAs photodiode at maximum P_{abs}: (a) shortest single Q-switched pulses for the applied OCs; (b) corresponding pulse train for T_{OC} = 9%.

The oscilloscope traces of the shortest single Q-switched pulses are shown in Fig. 6(a). The pulses exhibit a Gaussian temporal shape. The corresponding pulse train for T_{OC} = 9% measured at the maximum P_{abs} = 352 mW is shown in Fig. 6(b). The intensity fluctuations are <20% and they are mostly attributed to heating of the SA by non-

Optics EXPRESS

absorbed pump power [21]. During PQS operation, no damage of the SWCNT-SA was observed.

In the previous studies of PQS Tm-doped waveguide lasers [11–13,22], see details in Table 1, "slow" (e.g., polycrystalline Cr^{2+}:ZnSe) and "fast" SAs (e.g., graphene, Bi_2Te_3 topological insulator (TI)) were used. These lead to the generation of relatively long pulses, from tens of ns to few μs, as well as low output power. Recently, using a similar Tm:KYW/KYW epitaxy, we achieved 195 ns/5.8 nJ pulses (average output power: 6.5 mW) using a chemical vapor deposition grown graphene-SA [23]. Also, very recently, a SWCNT-SA was employed in a PQS fs-laser-written Tm:$KLu(WO_4)_2$ channel waveguide laser generating shorter pulses (50 ns/7 nJ) while the output power (10.3 mW) and the slope efficiency (3.8%) were relatively low most probably because of moderate waveguide propagation losses [14]. Thus, the present study presents a record in output characteristics for PQS Tm^{3+}-doped waveguide lasers in terms of average output power and slope efficiency. This performance is attributed to the high fraction of the saturable losses for the SWCNT-SA as compared to graphene and TIs, as well as a relatively low saturation intensity of the SWCNT-SA [3].

Table 1. Output Characteristics of PQS Thulium Waveguide Lasers Reported So Far

Gain material	Geometry / fabrication*	SA	P_{out}, mW	η, %	$\Delta\tau$, ns	E_{out}, nJ	PRF, kHz	P_{peak}, mW	Ref.
Tm:ZBLAN	channel / fs	graphene	6	~5	2760	240	25	87	[12]
Tm:ZBLAN	channel / fs	Bi_2Te_3	16.3	1.3	1400	**370**	44.1	264	[22]
Tm:YAG	channel / fs	graphene	6.5	~2	<500	9.5	684	~20	[13]
Tm:KLuW	channel / fs	SWCNTs	10.3	3.8	**50**	7	**1480**	141	[14]
Tm:KYW	planar / LPE	graphene	6.5	9	195	5.8	1130	30	[23]
Tm:KYW	planar / LPE	Cr^{2+}:ZnS	1.2	~3	1200	120	10	100	[11]
Tm:KYW	planar / LPE	SWCNTs	**45.6**	**22.5**	83	33	1390	**395**	**

*fs – femtosecond direct laser writing; LPE – liquid phase epitaxy growth.

**This work.

4. Conclusion

SWCNT-SAs are very suitable for passive Q-switching of ~2 μm waveguide lasers as demonstrated by PQS of a 18 μm-thick 5 at.% Tm:$KY_{1-x-y}Gd_xLu_y(WO_4)_2/KY(WO_4)_2$ epitaxy as active medium. The Tm^{3+}-doped planar waveguide laser delivered sub-100 ns pulses (71-83 ns) at ~1 MHz repetition rates. The maximum average output power was ~46 mW, the slope efficiency 22.5% and the Q-switching conversion efficiency 29%. Further shortening of the laser pulses down to few tens of ns and power scaling are expected substituting the planar by a channel waveguide geometry and using butt-coupled laser mirrors. Deposition of the SWCNTs on top of the waveguide for evanescent field interaction might further reduce the losses in the cavity.

Funding

Spanish Government (MAT2016-75716-C2-1-R (AEI/FEDER,UE), TEC 2014-55948-R); Generalitat de Catalunya (2014SGR1358); National Research Foundation of Korea (2016R1A2A1A05005381, 2017R1A4A1015426) .

Acknowledgments

E. K. acknowledges financial support from the Generalitat de Catalunya under grants 2016FI_B00844 and 2017FI_B100158. F. D. acknowledges additional support through the ICREA academia award 2010ICREA-02 for excellence in research. P. L. acknowledges financial support from the Government of the Russian Federation (Grant No. 074-U01) through ITMO Post-Doctoral Fellowship scheme.